Electronic supplementary materials

For: https://doi.org/10.1631/jzus.A2200340

General variational solution for seismic and static active earth pressure on rigid walls considering soil tensile strength cut-off

Shiguo XIAO[1,2], Yuan QI[2], Pan XIA[3]

[1]*Key Laboratory of High-speed Railway Engineering, Ministry of Education, Southwest Jiaotong University, Chengdu 610031, China*

[2]*School of Civil Engineering, Southwest Jiaotong University, Chengdu 610031, China*

[3]*Department of Geological Engineering, Southwest Jiaotong University, Chengdu 610031, China*

S1 Derivation of formula

Firstly, Eq. (12) may be simplified to $\partial m/\partial\sigma=0$ since σ' is not included in the expressions of m shown in Eqs. (10a) to (10c), namely, m is independent of σ' (Baker and Garber, 1978). So there is

$$y' = \frac{\tan\varphi(\lambda_2 y - \lambda_1) - (1 + \lambda_2 x)}{\tan\varphi(1 + \lambda_2 x) + (\lambda_2 y - \lambda_1)} \tag{S1}$$

As for Eq. (S1), there are two solutions of λ_2 in mathematics. Namely, $\lambda_2 = 0$ and $\lambda_2 \neq 0$, which substantially means Eq. (3) is omitted and considered, respectively.

Under the condition of $\lambda_2 = 0$, one can get

$$y' = \frac{-\lambda_1\tan\varphi - 1}{\tan\varphi - \lambda_1} \tag{S2}$$

So, Eq. (S2) indicates y' is invariable, which naturally means the failure surface is planar. Substituting Eq. (S2) into Eq. (13), we can obtain the expression of the function m, and get the formula of normal stress σ in light of Eq. (12). Then, as per Eq. (11), we can obtain the functional formula of E_a and solve it using the extremum principle. As the process is fairly clear and simple, the related formulas are not elaborated herein. Actually, the planar failure may be mathematically considered as a special case of curved failures. Thus, the demonstration emphasis in this paper becomes the case of $\lambda_2 \neq 0$ related closely to the soil nonplanar failure modes.

Presenting a polar coordinate system with a variable pole O_c (x_c, y_c) and transferring the rectangular to the polar coordinate system (see Fig. 1), we can get

$$x = -\frac{1}{\lambda_2} + r(\theta)\sin\theta = x_c + r(\theta)\sin\theta \tag{S3}$$

$$y = \frac{\lambda_1}{\lambda_2} - r(\theta)\cos\theta = y_c - r(\theta)\cos\theta \tag{S4}$$

where r and θ are radius and angular coordinate counterclockwise with reference to the pole $\mathbf{O}_c$ in the polar coordinate system, respectively.

Then substituting Eqs. (S3) and (S4) into Eq. (S1), one can get

$$\frac{\mathrm{d}r}{\mathrm{d}\theta} = -r\tan\varphi \tag{S5}$$

The solution of Eq. (S5) is

$$r(\theta) = K_1\,\mathrm{e}^{-\theta\tan\varphi} \tag{S6}$$

Eq. (S6) designates the critical sliding surface is log-spiral and the coordinates of the rotation center $\mathbf{O}_c$ are

$$\begin{cases} x_c = -\dfrac{1}{\lambda_2} \\ y_c = \dfrac{\lambda_1}{\lambda_2} \end{cases} \tag{S7}$$

Secondly, substituting Eq. (10) into Eq. (13), one can get

$$\begin{gathered}\frac{\partial m}{\partial y} - \frac{\mathrm{d}}{\mathrm{d}x}\left(\frac{\partial m}{\partial y'}\right) = -\sigma'(x)\left[\tan\varphi(\lambda_2 x + 1) + (\lambda_2 y - \lambda_1)\right] - 2\lambda_2\sigma(x)\tan\varphi - 2c\lambda_2 + \\ (1 + k_v)\gamma(\lambda_2 x + 1) - k_h\gamma(\lambda_2 y - \lambda_1)\end{gathered} \tag{S8}$$

Substituting Eqs. (S3) and (S4) into Eq. (S8), there is

$$\frac{\mathrm{d}\sigma}{\mathrm{d}\theta}-2\sigma\tan\varphi-2c+(1+k_{\mathrm{v}})\gamma r(\theta)\sin\theta+k_{\mathrm{h}}\gamma r(\theta)\cos\theta=0 \tag{S9}$$

As a result, the solution of Eq. (S9) is

$$\sigma(\theta)=\frac{K_1\gamma}{1+9\tan^2\varphi}\mathrm{e}^{-\theta\tan\varphi}\left[(1+k_{\mathrm{v}})(\cos\theta+3\tan\varphi\sin\theta)-k_{\mathrm{h}}(\sin\theta-3\tan\varphi\cos\theta)\right]-\frac{c}{\tan\varphi}+K_2\,\mathrm{e}^{2\theta\tan\varphi} \tag{S10}$$

Then, substituting Eqs. (S6) and (S10) into Eqs. (6) to (8), one can get

$$\begin{aligned}\overline{\mathrm{H}}=&\left\{\begin{aligned}&(1+k_{\mathrm{v}})\frac{K_1{}^2\gamma}{1+9u^2}\mathrm{e}^{-2u\theta}(\tan\varphi\sin2\theta-\frac{3\tan^2\varphi-1}{4}\cos2\theta+\frac{3\tan^2\varphi+3}{4})\\&-\frac{K_1c}{\tan\varphi}\mathrm{e}^{-\theta\tan\varphi}\cos\theta+K_1K_2\,\mathrm{e}^{\theta\tan\varphi}(\cos\theta-\tan\varphi\sin\theta)\\&+k_{\mathrm{h}}\frac{K_1{}^2\gamma}{1+9\tan^2\varphi}\mathrm{e}^{-2\theta\tan\varphi}(\tan\varphi\cos2\theta-\frac{1+3\tan^2\varphi}{2}\sin2\theta+2\tan\varphi)+k_{\mathrm{h}}y_{\mathrm{c}}K_1\gamma\mathrm{e}^{-\theta\tan\varphi}\sin\theta\end{aligned}\right\}_{\theta_{\mathrm{O}}}^{\theta_{\mathrm{M}}}\\&-k_{\mathrm{h}}\gamma\left[\frac{\tan\beta}{2}x_{\mathrm{M}}^2+H(1+\frac{\tan\beta}{\tan\alpha})x_{\mathrm{M}}\right]-k_{\mathrm{h}}(iG_{\mathrm{n}}+F_{\mathrm{q}})+E_{\mathrm{a}}\sin(\alpha-\delta)\\&-jk_{\mathrm{h}}\gamma\left[\frac{H^2}{\tan\alpha}(1+\frac{\tan\beta}{\tan\alpha})-\frac{H^2\tan\beta}{2\tan^2\alpha}-\frac{H^2}{2\tan\alpha}\right]=0\end{aligned} \tag{S11}$$

$$\begin{aligned}\overline{\mathrm{V}}=&\left\{\begin{aligned}&(1+k_{\mathrm{v}})\frac{K_1{}^2\gamma}{1+9\tan^2\varphi}\mathrm{e}^{-2\theta\tan\varphi}(-\tan\varphi\cos2\theta-3\tan^2\varphi\sin2\theta+2\tan\varphi)\\&-\frac{K_1c}{\tan\varphi}\mathrm{e}^{-\theta\tan\varphi}\sin\theta+K_1K_2\,\mathrm{e}^{\theta\tan\varphi}(\sin\theta+\tan\varphi\cos\theta)+(1+k_{\mathrm{v}})y_{\mathrm{c}}K_1\gamma\,\mathrm{e}^{-\theta\tan\varphi}\sin\theta\\&+k_{\mathrm{h}}\frac{K_1{}^2\gamma}{1+9\tan^2\varphi}\mathrm{e}^{-2\theta\tan\varphi}(\frac{1-3\tan^2\varphi}{4}\cos2\theta+\tan\varphi\sin2\theta-\frac{3\tan^2\varphi+3}{4})\end{aligned}\right\}_{\theta_{\mathrm{O}}}^{\theta_{\mathrm{M}}}\\&-(1+k_{\mathrm{v}})\left\{F_{\mathrm{q}}+iG_n+\gamma\left[\frac{\tan\beta}{2}x_{\mathrm{M}}^2+H(1+\frac{\tan\beta}{\tan\alpha})x_{\mathrm{M}}\right]\right\}+E_{\mathrm{a}}\cos(\alpha-\delta)\\&-j(1+k_{\mathrm{v}})\gamma\left[\frac{H^2}{\tan\alpha}(1+\frac{\tan\beta}{\tan\alpha})-\frac{H^2\tan\beta}{2\tan^2\alpha}-\frac{H^2}{2\tan\alpha}\right]=0\end{aligned} \tag{S12}$$

$$
\begin{aligned}
\overline{\mathrm{M}}=&\left\{\begin{aligned}
&\frac{K_1 c}{\tan\varphi}\mathrm{e}^{-\theta\tan\varphi}(y_\mathrm{c}\cos\theta-x_\mathrm{c}\sin\theta)+K_1K_2\,\mathrm{e}^{\theta\tan\varphi}\left[x_\mathrm{c}(\sin\theta+\tan\varphi\cos\theta)+y_\mathrm{c}(\tan\varphi\sin\theta-\cos\theta)\right]-\frac{K_1^{\,2}c}{2\tan\varphi}\mathrm{e}^{-2\theta\tan\varphi}\\
&+(1+k_\mathrm{v})\left\{\begin{aligned}
&K_1x_\mathrm{c}y_\mathrm{c}\gamma\mathrm{e}^{-\theta\tan\varphi}\sin\theta+K_1^{\,3}\gamma\mathrm{e}^{-3\theta\tan\varphi}\left[\frac{(1-3\tan^2\varphi)\cos\theta}{4(1+9\tan^2\varphi)}+\frac{\cos3\theta}{12}+\frac{\tan\varphi\sin\theta}{1+9\tan^2\varphi}\right]\\
&+\frac{K_1^{\,2}\gamma}{1+9\tan^2\varphi}\mathrm{e}^{-2\theta\tan\varphi}\left[(2\tan\varphi x_\mathrm{c}+\frac{3\tan^2\varphi-1}{2}y_\mathrm{c})-(3x_\mathrm{c}\tan^2\varphi+y_\mathrm{c}\tan\varphi)\sin2\theta-(x_\mathrm{c}\tan\varphi+\frac{3\tan^2\varphi+1}{2}y_\mathrm{c})\cos2\theta\right]
\end{aligned}\right\}\\
&+k_\mathrm{h}\left\{\begin{aligned}
&-\frac{1}{2}K_1y_\mathrm{c}^2\gamma\mathrm{e}^{-\theta\tan\varphi}\sin\theta-K_1^{\,3}\gamma\mathrm{e}^{-3\theta\tan\varphi}\left[\frac{\sin\theta}{3(1+9\tan^2\varphi)}+\frac{\cos^2\theta\sin\theta}{6}-\frac{\tan\varphi\cos\theta}{1+9\tan^2\varphi}\right]\\
&+\frac{K_1^{\,2}\gamma}{1+9\tan^2\varphi}\mathrm{e}^{-2\theta\tan\varphi}\left[(-\frac{3\tan^2\varphi+3}{4}x_\mathrm{c}-2y_\mathrm{c}\tan\varphi)+(x_\mathrm{c}\tan\varphi+\frac{1+3\tan^2\varphi}{2}y_\mathrm{c})\sin2\theta+(\frac{1-3\tan^2\varphi}{4}x_\mathrm{c}-y_\mathrm{c}\tan\varphi)\cos2\theta\right]
\end{aligned}\right\}
\end{aligned}\right\}_{\theta_\mathrm{O}}^{\theta_\mathrm{M}}\\
&-(1+k_\mathrm{v})\left\{M_\mathrm{qv}-iM_\mathrm{nv}+\gamma\left\{\frac{\tan\beta x_\mathrm{M}^3}{3}+\frac{H}{2}(1+\frac{\tan\beta}{\tan\alpha})x_\mathrm{M}^2+j\left[\frac{H^3\tan\beta}{3\tan^3\alpha}-\frac{H^3}{2\tan^2\alpha}(1+\frac{\tan\beta}{\tan\alpha})+\frac{H^3}{3\tan^2\alpha}\right]\right\}\right\}\\
&+k_\mathrm{h}\left\{\frac{\gamma}{2}\left[\frac{\tan^2\beta x_\mathrm{M}^3}{3}+H(\tan\beta+\frac{\tan^2\beta}{\tan\alpha})x_\mathrm{M}^2+H^2(1+\frac{\tan\beta}{\tan\alpha})^2x_\mathrm{M}\right]+iM_\mathrm{nh}+M_\mathrm{qh}\right\}\\
&+jk_\mathrm{h}\frac{\gamma}{2}\left[\frac{H^3\tan^2\beta}{3\tan^3\alpha}-H^3(\frac{\tan\beta}{\tan^2\alpha}+\frac{\tan^2\beta}{\tan^3\alpha})+\frac{H^3}{\tan\alpha}(1+\frac{\tan\beta}{\tan\alpha})^2-\frac{H^3}{3\tan\alpha}\right]-E_\mathrm{a}\left[\sin(\alpha-\delta)z_\mathrm{a}+\cos(\alpha-\delta)\frac{z_\mathrm{a}}{\tan\alpha}\right]=0
\end{aligned}
\tag{S13}
$$

where j is another calculation index related to dip angle of wall back and it is equal to 0 if α is not more than 90 degrees. Conversely, it is equal to 1.

In light of the geometric relationships between the polar and rectangular coordinate system as well as boundary conditions of the segment of the slip surface **MO**, there are

$$x_\mathrm{c}+K_1\,\mathrm{e}^{-\theta_\mathrm{O}\tan\varphi}\sin\theta_\mathrm{O}=0 \tag{S14}$$

$$y_\mathrm{c}-K_1\,\mathrm{e}^{-\theta_\mathrm{O}\tan\varphi}\cos\theta_\mathrm{O}=0 \tag{S15}$$

$$x_\mathrm{M}-x_\mathrm{c}-K_1\,\mathrm{e}^{-\theta_\mathrm{M}\tan\varphi}\sin\theta_\mathrm{M}=0 \tag{S16}$$

$$y_\mathrm{c}-K_1\,\mathrm{e}^{-\theta_\mathrm{M}\tan\varphi}\cos\theta_\mathrm{M}=H+(x_\mathrm{M}+\frac{H}{\tan\alpha})\tan\beta-d \tag{S17}$$

Besides, according to basic principles of variational calculus method, the cross-sectional condition at point **M** is (Giaquinta and Hildebrandt, 2004)

$$\left[m+(s'-d'-y')\frac{\partial m}{\partial y'}\right]_{x=x_\mathrm{M}}=0 \tag{S18}$$

For the same soil, vertical crack depth d can be assumed as an independent variable of x according to Rankine-Bell relationship of active earth pressure (Bell, 1915). Therefore, one can get

$$\left[m+(s'-y')\frac{\partial m}{\partial y'}\right]_{x=x_{\mathrm{M}}}=0 \tag{S19}$$

In the condition of a planar surface of the backfill, the function $g(x)$ to generally express the soil surface **AB** can be simply written as

$$g(x)=x\tan\beta+H(1+\frac{\tan\beta}{\tan\alpha}) \tag{S20}$$

Then, the simplified surface function $s(x)$ can be expressed as

$$s=\begin{cases} s_{\mathrm{i=1}}=g(x)=x\tan\beta+H(1+\dfrac{\tan\beta}{\tan\alpha}) \quad ,x\in\left[0,x_{\mathrm{M}}\right] \\ s_{\mathrm{i=0}}=\begin{cases} -\tan\alpha\cdot x & ,x\in\left[0,-\dfrac{H}{\tan\alpha}\right] \\ g(x)=x\tan\beta+H(1+\dfrac{\tan\beta}{\tan\alpha}), & x\in\left(-\dfrac{H}{\tan\alpha},x_{\mathrm{M}}\right] \end{cases} \end{cases} \tag{S21}$$

Hence, substituting Eqs. (10), (S10), and (S21) into Eq. (S19), we can get

$$\begin{aligned}
&\left\{\frac{K_1\gamma}{1+9\tan^2\varphi}\mathrm{e}^{-\theta_{\mathrm{M}}\tan\varphi}\left[(1+k_{\mathrm{v}})(\cos\theta_{\mathrm{M}}+3\tan\varphi\sin\theta_{\mathrm{M}})-k_{\mathrm{h}}(\sin\theta_{\mathrm{M}}-3\tan\varphi\cos\theta_{\mathrm{M}})\right]-\frac{c}{\tan\varphi}+K_2\,\mathrm{e}^{2\theta_{\mathrm{M}}\tan\varphi}\right\} \\
&\cdot\left[\tan\varphi(\cos\theta_{\mathrm{M}}+\tan\beta\sin\theta_{\mathrm{M}})+\sin\theta_{\mathrm{M}}-\tan\beta\cos\theta_{\mathrm{M}}\right]+c(\cos\theta_{\mathrm{M}}+\tan\beta\sin\theta_{\mathrm{M}}) \\
&-(1+k_{\mathrm{v}})((q+\gamma d)\sin\theta_{\mathrm{M}}+\frac{(1+k_{\mathrm{v}})\left[\frac{q}{2}(\frac{H}{\tan\rho}-a)^2+q(\frac{H}{\tan\rho}-a)x_{\mathrm{c}}+iG_{\mathrm{n}}x_{\mathrm{c}}+iM_{\mathrm{nv}}\right]}{K_1\,\mathrm{e}^{-\theta_{\mathrm{M}}\tan\varphi}x_{\mathrm{M}}} \\
&+\frac{k_h\left[\gamma d(-K_1\,\mathrm{e}^{-\theta_{\mathrm{M}}\tan\varphi}\cos\theta_{\mathrm{M}}+\frac{1}{2}d)+qH(1+\frac{\tan\beta}{\tan\alpha})+qx_{\mathrm{M}}\tan\beta-qy_{\mathrm{c}}\right]}{K_1\,\mathrm{e}^{-\theta_{\mathrm{M}}\tan\varphi}} \\
&+\frac{k_h\left[iM_{\mathrm{nh}}+\frac{q\tan\beta}{2}(\frac{H^2}{\tan^2\alpha}-a^2)+qH(\frac{H}{\tan\alpha}-a)-q(\frac{H}{\tan\alpha}-a)y_{\mathrm{c}}-iG_{\mathrm{n}}y_{\mathrm{c}}\right]}{K_1\,\mathrm{e}^{-\theta_{\mathrm{M}}\tan\varphi}x_{\mathrm{M}}}=0
\end{aligned} \tag{S22a}$$

$$\begin{aligned}
&\left\{\frac{K_1\gamma}{1+9\tan^2\varphi}\mathrm{e}^{-\theta_{\mathrm{M}}\tan\varphi}\left[(1+k_{\mathrm{v}})(\cos\theta_{\mathrm{M}}+3\tan\varphi\sin\theta_{\mathrm{M}})-k_{\mathrm{h}}(\sin\theta_{\mathrm{M}}-3\tan\varphi\cos\theta_{\mathrm{M}})\right]-\frac{c}{\tan\varphi}+K_2\,\mathrm{e}^{2\theta_{\mathrm{M}}\tan\varphi}\right\} \\
&\cdot\left[\tan\varphi(\cos\theta_{\mathrm{M}}+\tan\beta\sin\theta_{\mathrm{M}})+\sin\theta_{\mathrm{M}}-\tan\beta\cos\theta_{\mathrm{M}}\right]+c(\cos\theta_{\mathrm{M}}+\tan\beta\sin\theta_{\mathrm{M}}) \\
&-(1+k_{\mathrm{v}})\gamma d\sin\theta_{\mathrm{M}}+\frac{k_h\gamma d}{K_1\,\mathrm{e}^{-\theta_{\mathrm{M}}\tan\varphi}}(-K_1\,\mathrm{e}^{-\theta_{\mathrm{M}}\tan\varphi}\cos\theta_{\mathrm{M}}+\frac{1}{2}d) \\
&-\frac{1}{K_1\,\mathrm{e}^{-\theta_{\mathrm{M}}\tan\varphi}x_{\mathrm{M}}}\left[(1+k_{\mathrm{v}})(-iM_{\mathrm{nv}}-iG_{\mathrm{n}}x_{\mathrm{c}})-k_h(iM_{\mathrm{nh}}-iG_{\mathrm{n}}y_{\mathrm{c}})\right]=0
\end{aligned} \tag{S22b}$$

$$\begin{aligned}
&\left\{\frac{K_1\gamma}{1+9\tan^2\varphi}e^{-\theta_M\tan\varphi}\left[(1+k_v)(\cos\theta_M+3\tan\varphi\sin\theta_M)-k_h(\sin\theta_M-3\tan\varphi\cos\theta_M)\right]-\frac{c}{\tan\varphi}+K_2e^{2\theta_M\tan\varphi}\right\}\\
&\cdot\left[\tan\varphi(\cos\theta_M+\tan\beta\sin\theta_M)+\sin\theta_M-\tan\beta\cos\theta_M\right]+c(\cos\theta_M+\tan\beta\sin\theta_M)\\
&-(1+k_v)\gamma d\sin\theta_M+\frac{k_h\gamma d}{K_1e^{-\theta_M\tan\varphi}}(-K_1e^{-\theta_M\tan\varphi}\cos\theta_M+\frac{1}{2}d)\\
&-\frac{1}{K_1e^{-\theta_M\tan\varphi}x_M}\left[(1+k_v)(M_{qv}-iM_{nv}-F_qx_c-iG_nx_c)-k_h(M_{qh}+iM_{nh}-F_qy_c-iG_ny_c)\right]=0
\end{aligned} \tag{S22c}$$

where the real conditions of Eqs. (S22a), (S22b) and (S22c) are $x_B \geq a\text{-}H/\tan\alpha+b$, $a\text{-}H/\tan\alpha < x_B < a\text{-}H/\tan\alpha+b$, and $x_B \leq a\text{-}H/\tan\alpha$, respectively.

Parameter study and discussion

(1) Cohesion of soil *c*, unit weight *γ* and wall height *H*

As shown in Fig. S1, K_a is almost linearly decreasing with the increase of the normalized cohesion $c/(\gamma H)$ as expected (Li & Yang, 2019). The minimum value of the ratio ξ is decreasing nonlinearly with the increase of $c/(\gamma H)$. Shear segment of the critical slip surface is always planar and gradually developing towards the wall as $c/(\gamma H)$ increases, but d/H is linearly increasing with $c/(\gamma H)$. Distribution of normal stress on the shear segment of the slip surface is still approximately linear with various values under different c.

S2 Soil internal friction angle *φ*

Fig. S2 shows K_a is nonlinearly reducing as φ increases, but the minimum value of the ratio ξ is almost not changed. The sliding surface develops gradually towards the wall as φ increases. Depth of the tension crack is approximately linearly increasing with the increase of φ. The normal stress σ is still of nearly linear distribution characteristics along the shear segment of the slip surface under different φ.

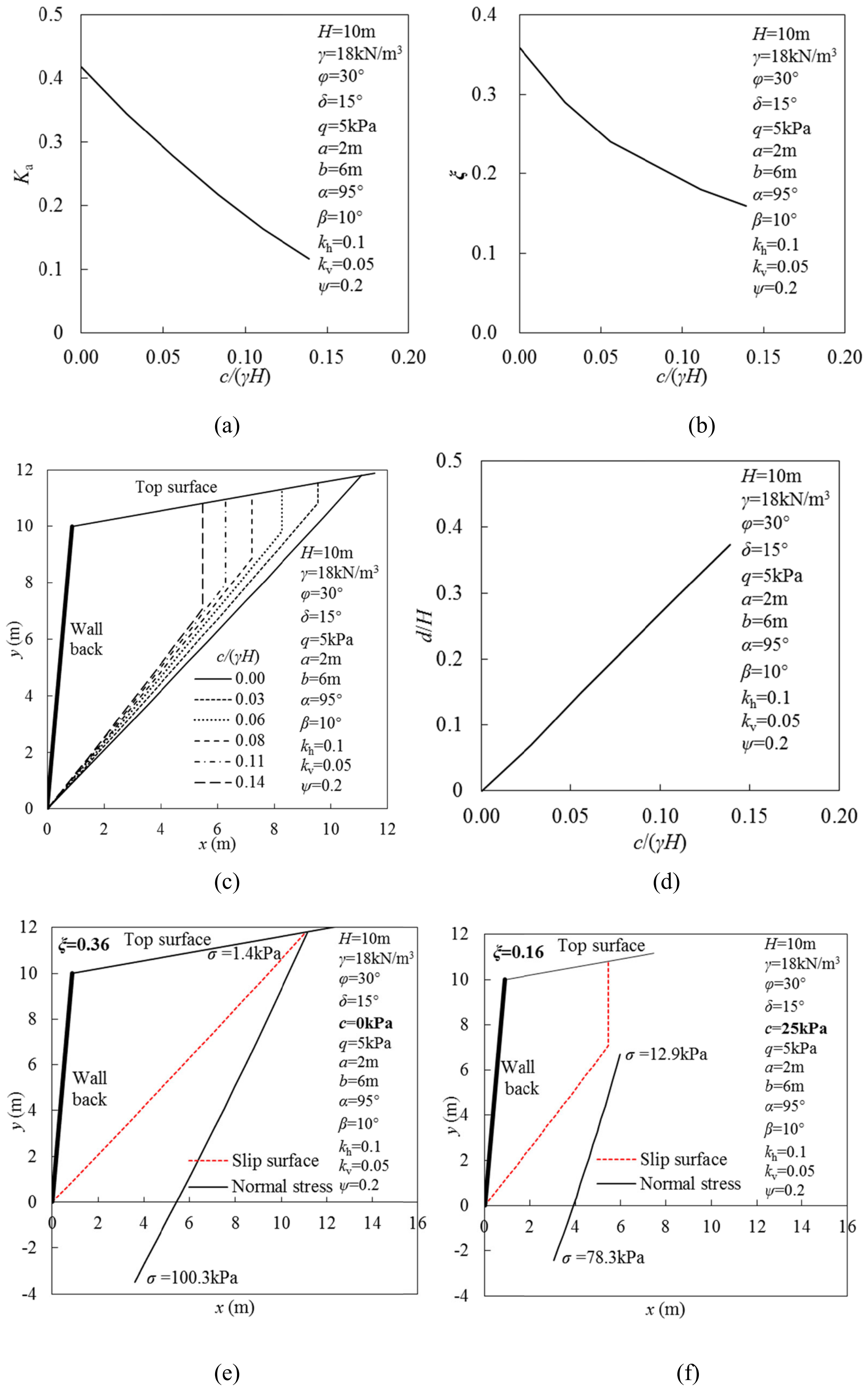

Fig. S1 Influences of soil cohesion on the active earth pressure and other related items (a) K_a vs. $c/(\gamma H)$; (b) ξ vs. $c/(\gamma H)$; (c) Slip surfaces; (d) d/H vs. $c/(\gamma H)$; (e) and (f) Distribution of normal stress on slip surface under $c/(\gamma H)$ = 0 and 0.139, respectively

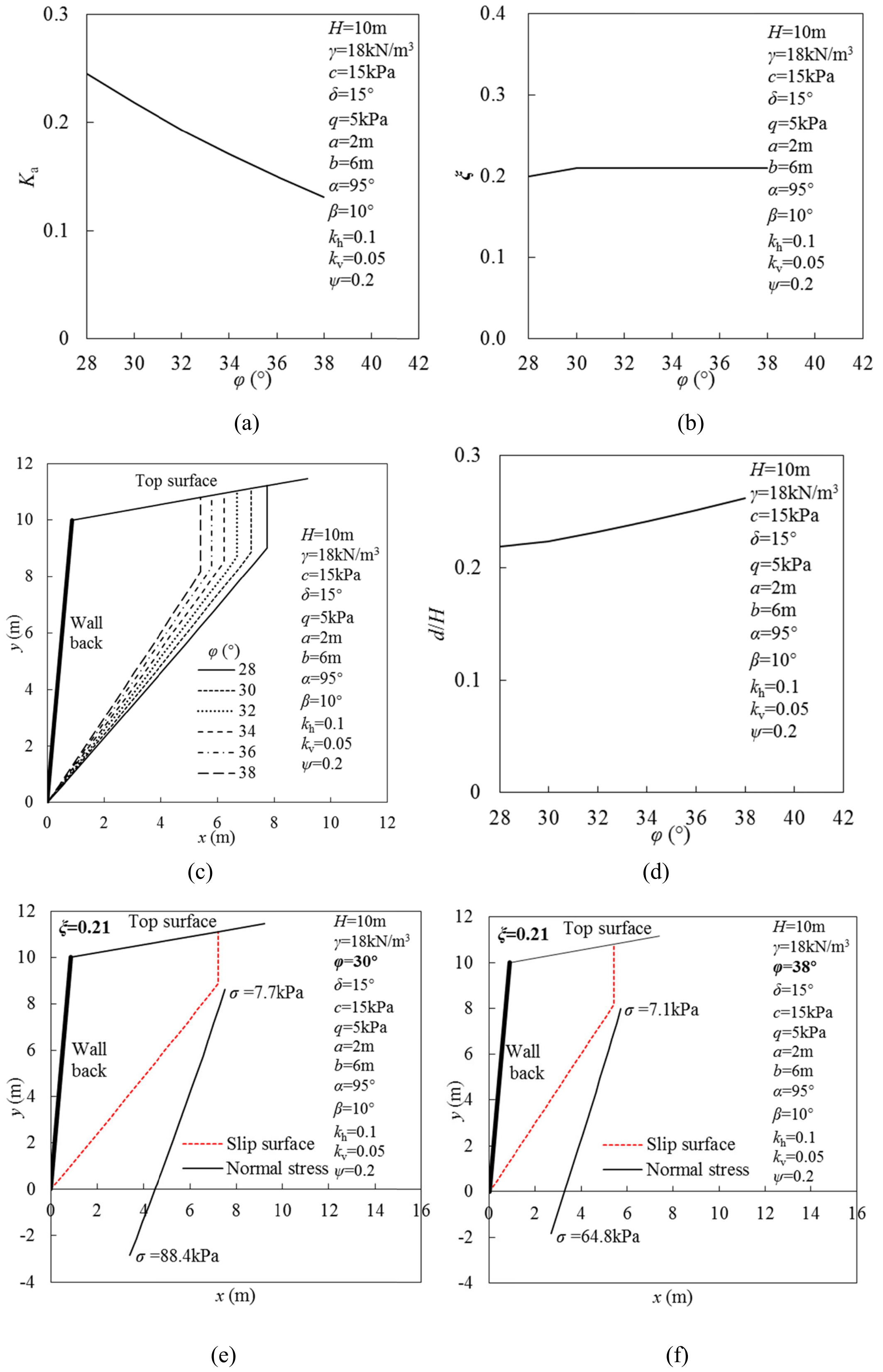

Fig. S2 Influences of φ on the active earth pressure and other related items (a) $K_{\mathbf{a}}$ vs. φ; (b) ξ vs. φ;

(c) Slip surfaces; (d) d/H vs. φ; (e) and (f) Distribution of normal stress on slip surface under φ = 30° and 38°, respectively

S3 Wall back dip angle *α*

Fig. S3 displays that K_a is decreasing linearly with the increase of α, and the minimum value of the ratio ξ is nearly linearly decreasing as α increases. The failure surface is influenced evidently by α, and it develops towards the wall as α increases within 90° and towards the soil interior with the increase of α over 90°. However, depth of tension crack is increasing nonlinearly with α. Additionally, it can be inferred from Fig. S3 (a) that if α reaches 123.44°, K_a can arrive at zero, which means there is possibly no active earth pressure on the wall if the inclination of wall back is large enough.

S4 Soil surface dip angle *β*

As shown in Fig. S4, K_a nonlinearly increases with β as expected, and the minimum value of the ratio ξ is almost not altered. The critical sliding surface grows towards the soil interior with β, and depth of tension crack is increasing approximately linearly as β increases.

S5 Strip surcharge *q*

Fig. S5 displays that K_a is linearly growing with $q/(\gamma H)$ as expected (Greco, 2006), but the minimum value of the ratio ξ decreases faintly. The shear slip segment of the failure surface cannot be influenced by $q/(\gamma H)$, but the tension failure segment of the slip surface is slightly moving far away from the wall. Normal stress on the shear slip segment is influenced to some degree by q, but its distribution still keeps approximately linear under different q.

S6 Horizontal offset distance of the surcharge *a*

Fig. S6 shows K_a is decreasing linearly as a/H increases within a certain range. If a/H reaches a high enough value, it has no influence on the earth thrust as expected. The minimum value of the ratio ξ is faintly changed with a/H. Additionally, the failure surface is scarcely influenced by a/H, but depth of tension crack is increasing to some extent with the increase of a/H in a limited range. The normal stress σ is influenced marginally by a, and the influence occurs particularly at the point of the wall heel under different a.

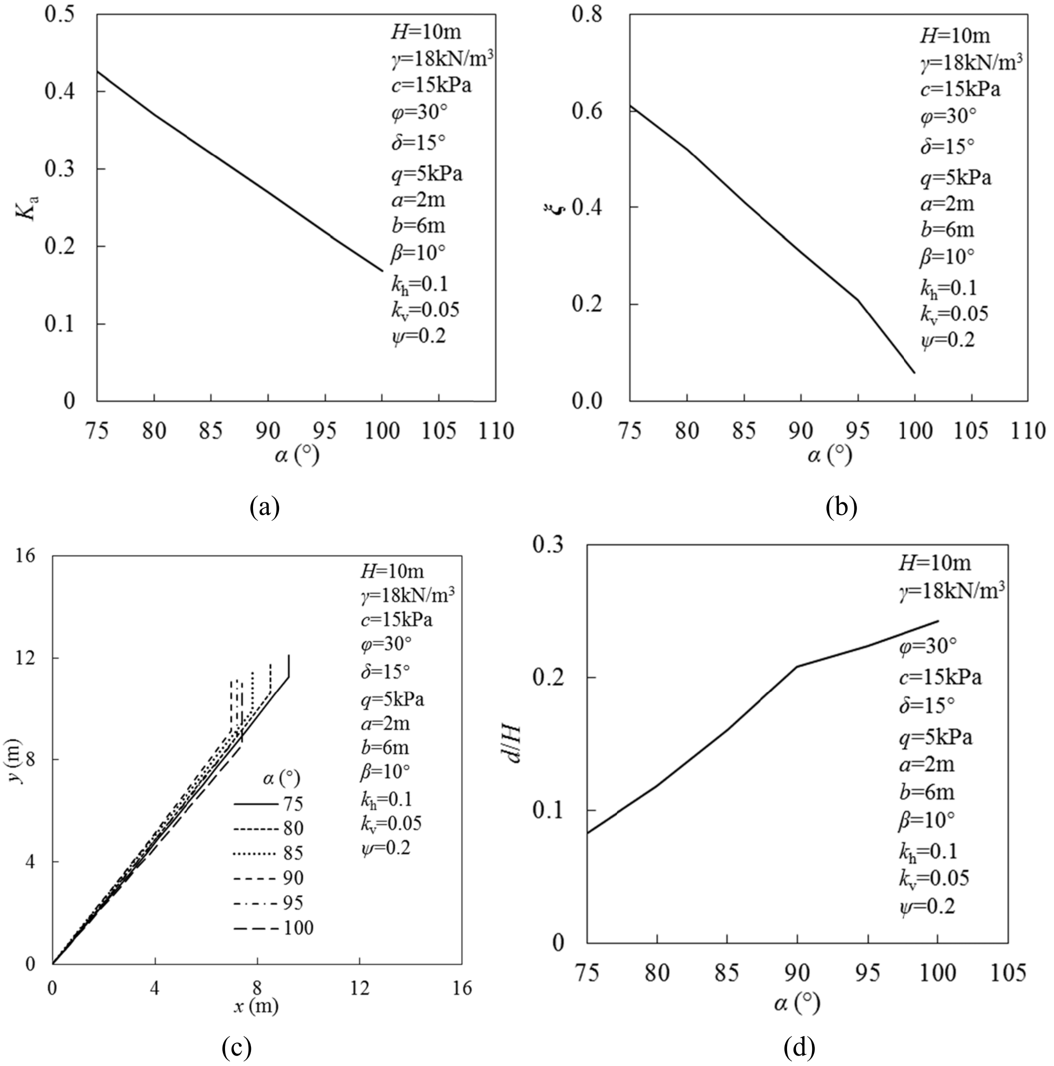

Fig. S3 Influences of α on the active earth pressure and other related items (a) K_a vs. α; (b) ξ vs. α; (c) Slip surfaces; (d) d/H vs. α

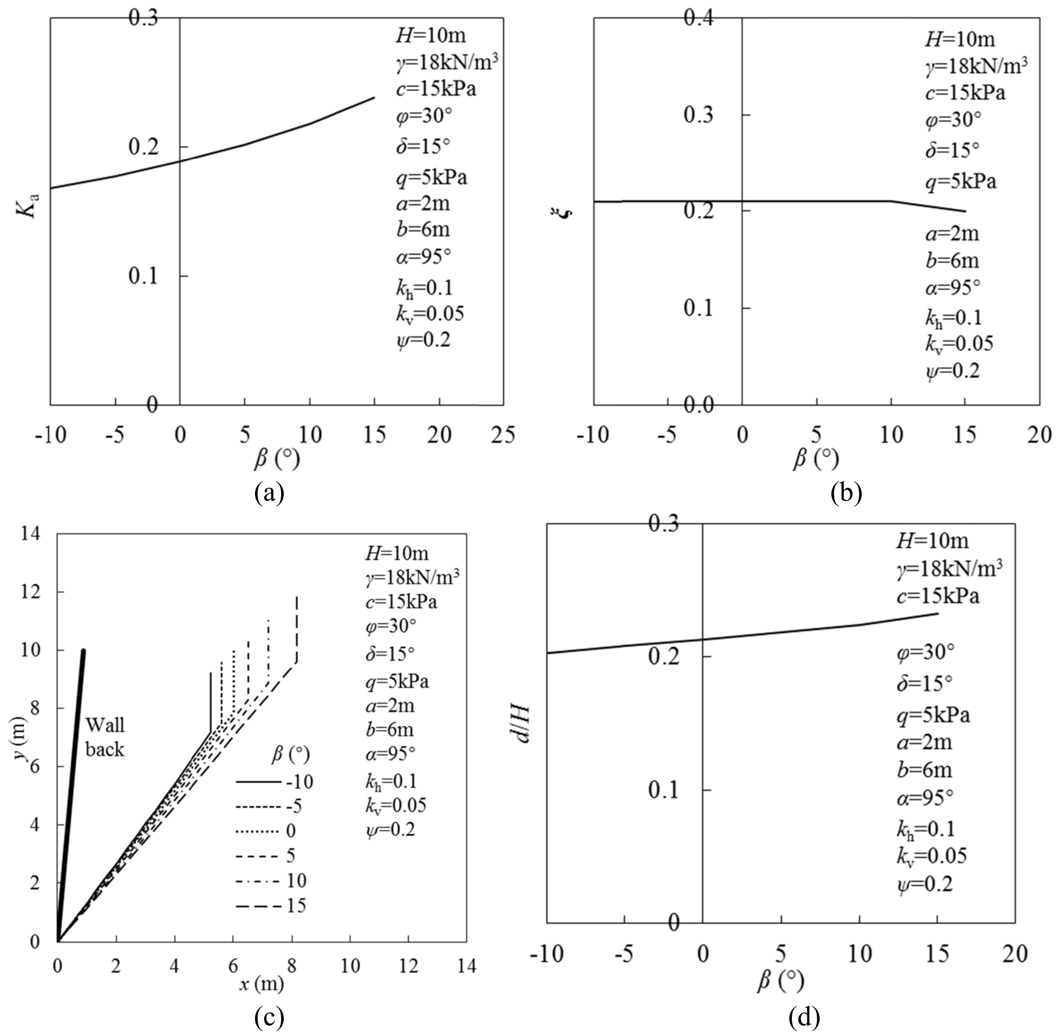

Fig. S4 Influences of β on the active earth pressure and other related items (a) K_a vs. β; (b) ξ vs. β; (c) Slip surfaces; (d) d/H vs. β

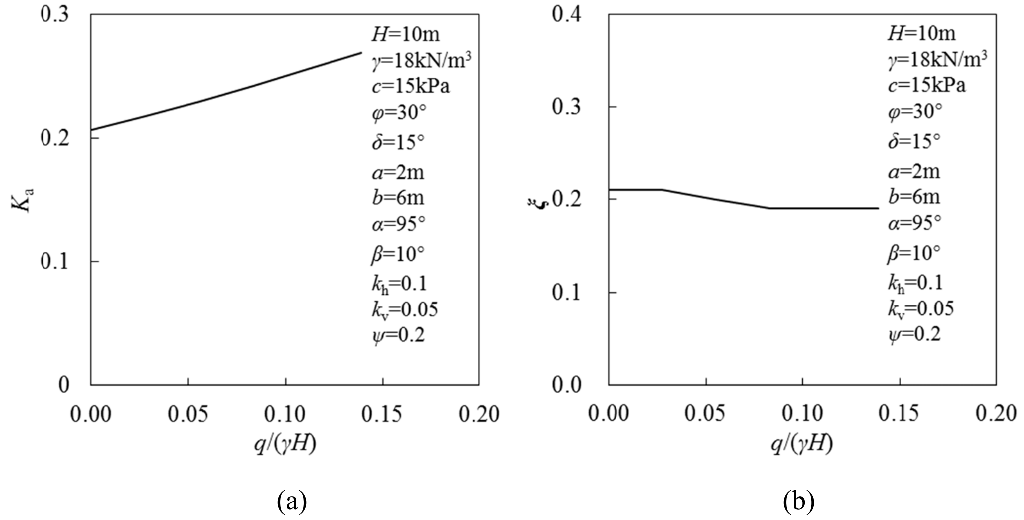

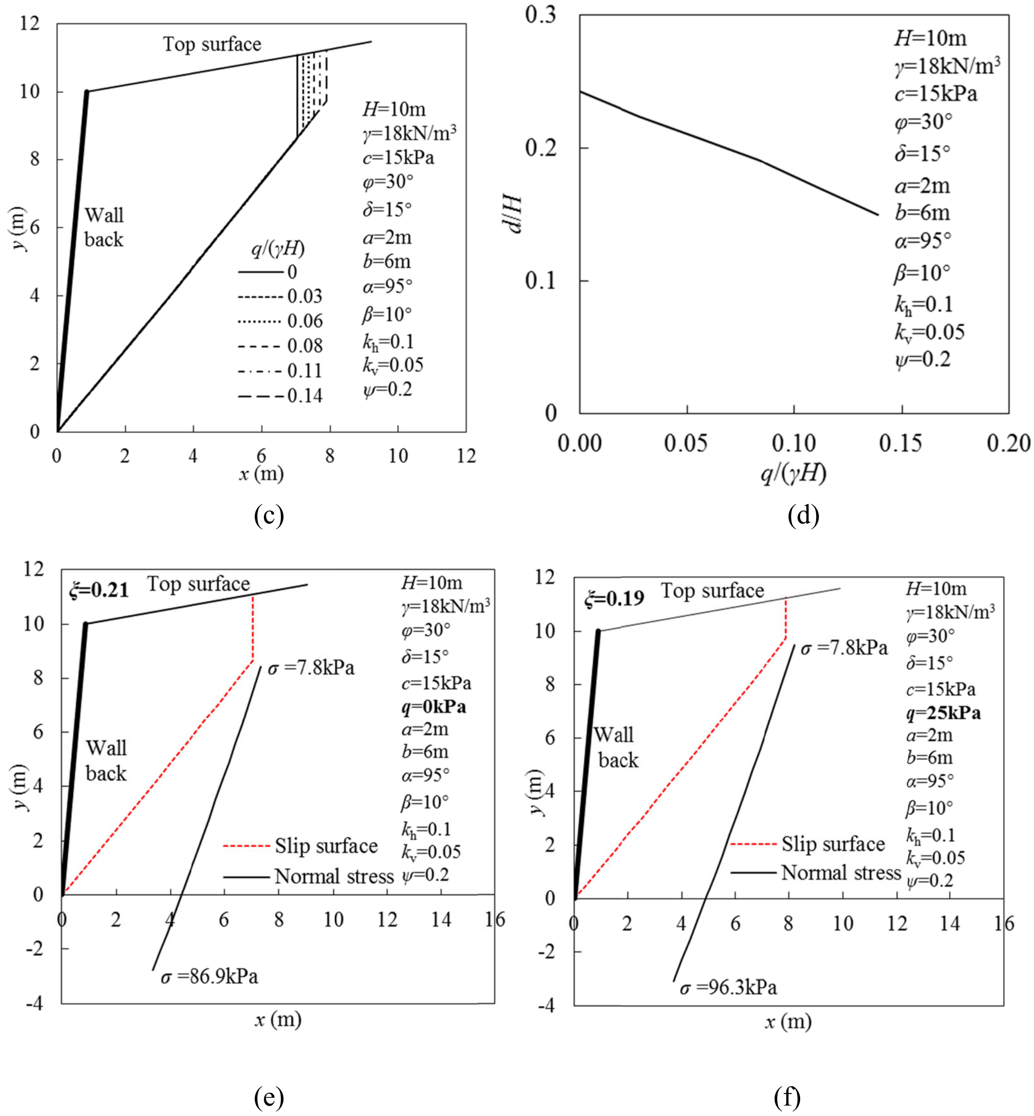

Fig. S5 Influences of q on the active earth pressure and other related items (a) K_a vs. $q/(\gamma H)$; (b) ξ vs. $q/(\gamma H)$; (c) Slip surfaces; (d) d/H vs. $q/(\gamma H)$; (e) and (f) Distribution of normal stress on slip surface under $q/(\gamma H)$ = 0 and 0.139, respectively

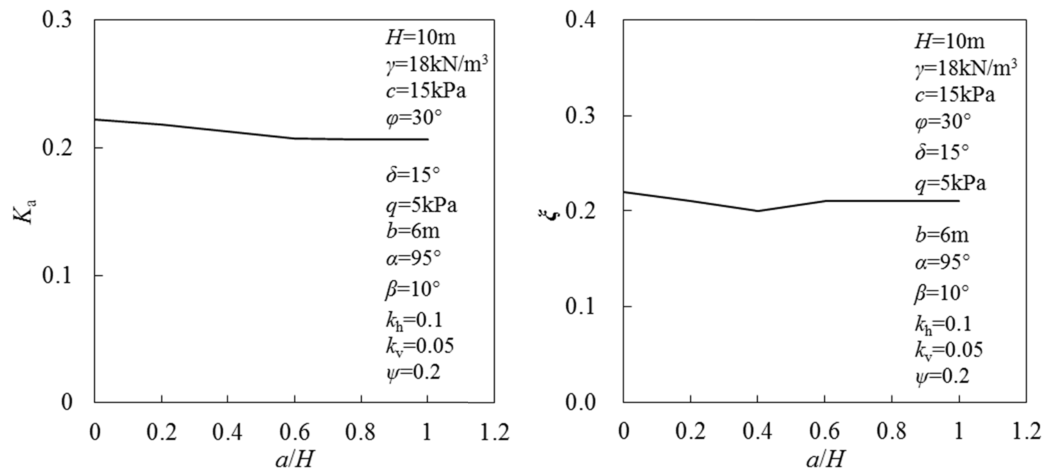

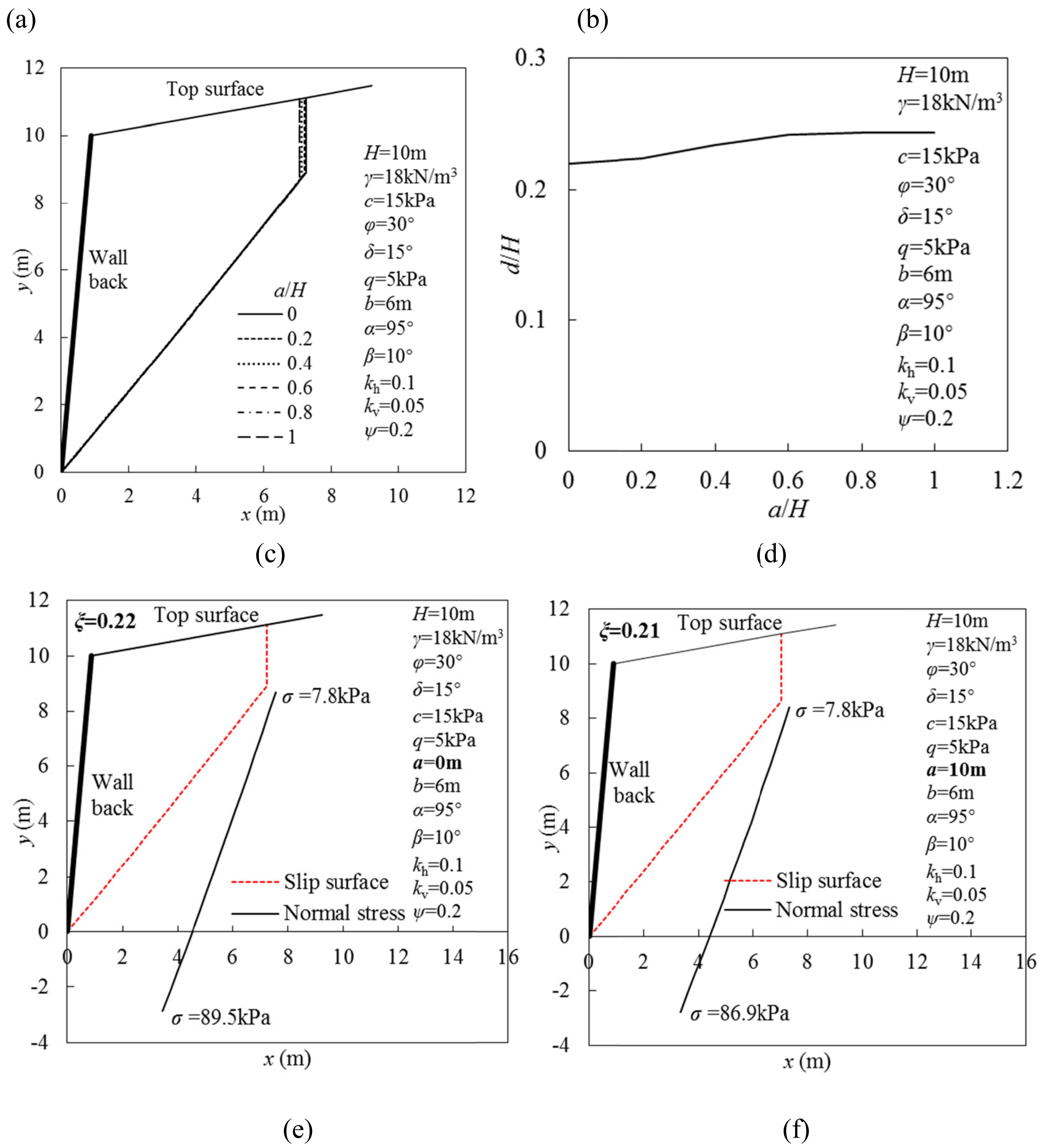

Fig. S6 Influences of a on the active earth pressure and other related items (a) K_a vs. a/H; (b) ξ vs. a/H; (c) Slip surfaces; (d) d/H vs. a/H; (e) and (f) Distribution of normal stress on slip surface under a/H = 0 and 1, respectively

S7 Distribution width of the surcharge *b*

As shown in Fig. S7, K_a is increasing linearly with the increase of b/H within a certain range. After b/H reaches a great value, it does not have any influences on the earth thrust as expected. Additionally, b/H has almost no effect on the minimum value of the ratio and critical slip surface, but depth of tension crack is decreasing as b/H increases in a limited range. b has almost no effect on the normal stress σ.

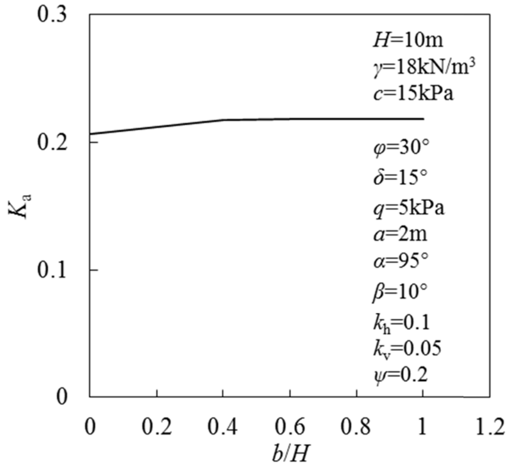

(a)

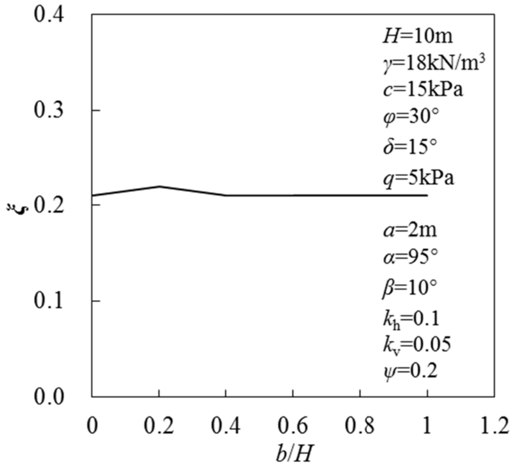

(b)

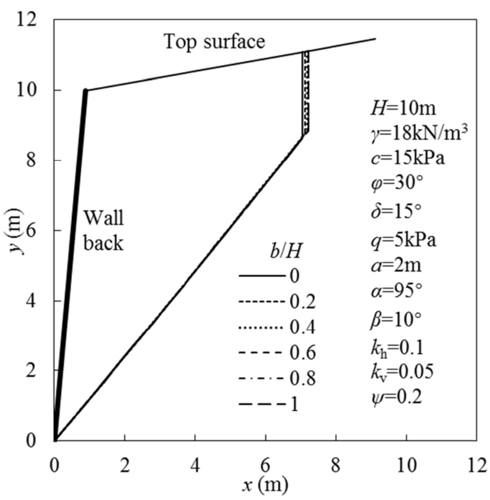

(c)

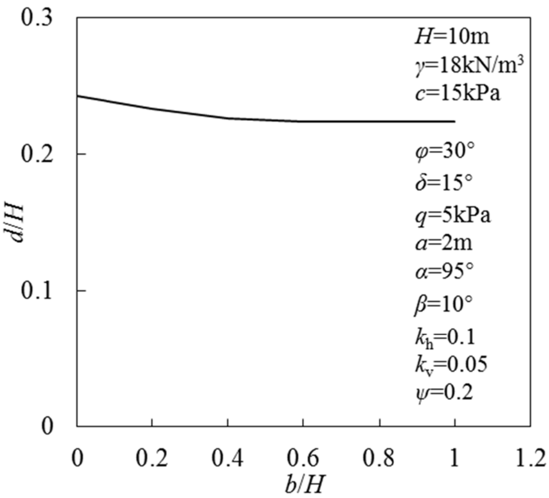

(d)

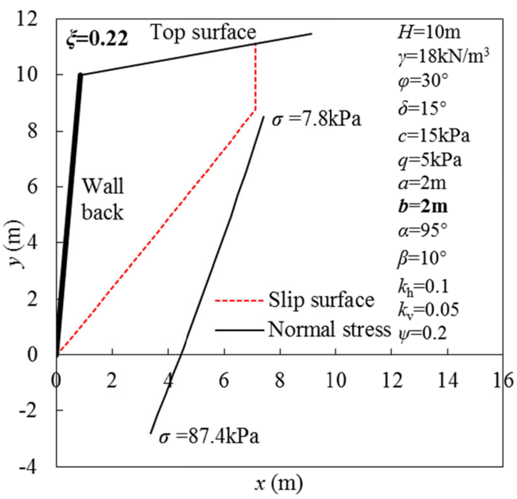

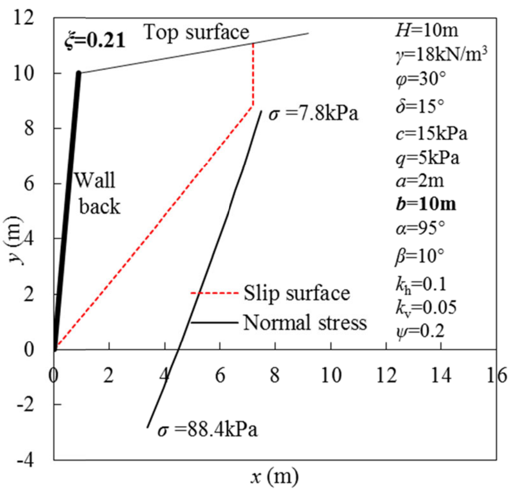

(e) (f)

Fig. S7 Influences of b on the active earth pressure and other related items (a) K_a vs. b/H; (b) ξ vs. b/H; (c) Slip surfaces; (d) d/H vs. b/H; (e) and (f) Distribution of normal stress on slip surface under $b/H = 0.2$ and 1, respectively